Available online at www.sciencedirect.com
ScienceDirect
Journal of Power Sources 179 (2008) 310–316
JOURNAL OF POWER SOURCES
www.elsevier.com/locate/jpowsour

Mechanism for electrochemical hydrogen insertion in carbonaceous materials

Deyang Qu *

Department of Chemistry, University of Massachusetts Boston, Boston, MA 02482, United States

Received 27 December 2007; accepted 31 December 2007
Available online 5 January 2008

Abstract

The mechanism for safe and reversible storage of hydrogen in porous carbonaceous materials by electrochemical decomposition of water in alkaline electrolyte is proposed. Atomic H was found to be inserted into the microdomains of defective graphene layers. Hydrogen storage capacity increases with increasing interlayer distance between carbon sheets. Hydrogen insertion in carbonaceous materials occurs at ambient conditions. Static potential acts as an electrochemical valve which can retain the hydrogen in the carbon structure, thus preventing leakage during storage.

Keywords: Energy conversion; Intercalations; Hydrogen storage; Porous carbon; Electrochemistry

1. Introduction

The replacement of fossil fuels with hydrogen, which can be produced from renewable sources and burn pollution free, could dramatically reduce the buildup of greenhouse gases which may cause severe climate change. Finding a safe, cheap and simple method to store hydrogen, together with producing hydrogen and converting it to electricity are two of the most daunting challenges facing scientists at the present time. Unfortunately, none of the existing H_2 storage methods – including hydrogen compression and liquefaction under cryogenic conditions, chemical and metal hydrides and gas-on-solid adsorption – satisfy all the criteria.

One way to increase volumetric hydrogen density to the level of liquid hydrogen under ambient conditions is the dissociation of hydrogen molecules in combination with a tight binding or electron transfer to the host material. The storage of electrochemically generated hydrogen has found a wide application in multi-component metal-hydride alloys. Many metals and alloys are able to reversibly store large amounts of hydrogen, and this system has been studied extensively over the past four decades [1–4]. Hydrogen filling can be done using molecular hydrogen gas, which is dissociated at the surface to become adsorbed H atoms, or adsorbed hydrogen atoms electrochemically generated from aqueous electrolytes. The adsorbed H atoms then diffuse into the matrix of the hydride material and reside in tetrahedral or octahedral interstitial sites. Upon release, the atomic hydrogen stored in the interstitial sites recombines at particle surface sites to form molecular hydrogen. However, most effective metal hydrides are made of relatively heavy elements such as Ni, Co and La, and the gravimetric capacity of regular hydrides is less than 2 wt.% [5], which is significantly lower than the Department of Energy (DOE)'s goal of 6.5 wt.%. Alloys with lighter elements, e.g. Mg [6,7], have also been investigated for a higher gravimetric storage capacity (3–7 wt.%), but for thermodynamic reasons, they only release hydrogen at a high temperature (>500 °C). The kinetic aspect of hydrogen release can be improved by nanostructuring and adding a catalyst, whereby the thermodynamics remain unchanged. Recently a new group of low to medium temperature chemical hydrides, nitrides and imides, including $MAlH_4$, MBH_4, Li_3N, etc., have attracted significant attention [8–12]. A large amount of hydrogen can be stored in these materials and with a catalyst, hydrogen can be released easily at almost ambient conditions. Despite these advantages, two major obstacles remain: firstly, the generation of hydrogen is irreversible and lengthy, and solvent-based synthetic processes may be involved to re-generate the compounds; secondly,

* Tel.: +1 617 287 6035; fax: +1 617 287 6185.
E-mail address: Deyang.qu@umb.edu.

0378-7753/$ – see front matter © 2008 Elsevier B.V. All rights reserved.
doi:10.1016/j.jpowsour.2007.12.098

significant volume change (15–25%) needs to be accommodated.

Metal-hydride alloys, which have been used for electrochemical hydrogen storage, are heavy, expensive and not stable. Due to the good electronic conductivity and light weight of carbon, hydrogen sorption during electro-decomposition of water on a cathodically polarized carbon electrode is an alternative and elegant method for hydrogen storage at an ambient temperature and pressure [13,14]. For hydrogen storage alloys, hydrogen atoms enter the metal lattice for the hydride (reduced) state [15]. Even though electrochemically formed hydrogen can be stored in carbon material [16], the mechanism is still under debate. Electrochemical methods have also been used as an alternative and effective method for storing hydrogen in carbonaceous materials at an ambient temperature and pressure [17]. In most of the studies, the electrodes contained nanotubes [18–21]. Due to poor conductivity, nanotubes are always a minor fraction mixing with other metallic conductive fillers, e.g. Ni (>90%) [19], Cu in the ratio of 1:3 [21], thus, the gravimetric capacity of nanotubes is significantly limited. Indeed, the practical value of nanotubular materials is dubious due to the cost, limited scale of production, and uncertain purity. Activated carbon and carbon fibers have been demonstrated as good candidates for electrochemical hydrogen storage [13,17,22,23]. However, the results reported in the literature are very inconclusive; for example, the double-layer contribution, which is significant for electrodes made with high surface area carbon material [24,25], was not corrected in many reports. Thus the calculated hydrogen storage based on discharge capacity is inflated. The proposed mechanisms for hydrogen storage, e.g. the adsorption of electrochemically generated molecular hydrogen in micro-pores [16] and the so-called "nascent-hydrogen" adsorbed on the surface of carbon [13], lack sufficient experimental support. The intercalation of hydrogen into the interlayer of carbon is believed to be prohibited [26], which was a highly questionable conclusion.

2. Experimental details

Ultra high surface area carbon materials were either obtained from carbon manufacturers or made in-house by modifying different precursor materials through various activation procedures in order to create various porosities and structures. Table 1 tabulates the surface area, average pore size, type and manufacture of the activated carbon materials used in the studies. All activated carbon materials were reflux-washed with acetone in a Soxhlet extractor for 48 h to remove most of the weakly bonded surface functional groups that remained from the precursors and the manufacturing process. All U-grade carbon materials were activated at 800–900 °C in steam mixing with various percentages of CO_2.

Aqueous potassium hydroxide solution (30 wt.%) was used as an electrolyte in all experiments at 298 ± 1 K. All potentials reported were referred to the Hg/HgO reference electrode immersed in KOH of the same concentration as the experimental electrolyte. Fig. 1 shows the electrochemical cell. A special Teflon electrode holder was used to accommodate and mount activated carbon electrodes. An electrode was made with 90 wt. of carbon and 10 wt.% of Teflon dry material. Teflon suspension (T-30) from DuPont was used. The activated carbon powder was first thoroughly mixed with T-30 in a high-speed Waring blender and the paste was left to air dry. The resulting Teflon-bonded carbon was hot-rolled into a thin film. The electrodes were then punched out of the film. When carbon cloth was used, the electrodes were just punched out of the cloth. Two pieces of carbon electrodes were sandwiched on a Pt current collector by the screw-fitting plug, and the electrode holder resided in the center of a large Pt-mesh net counter electrode to ensure homogeneous current distribution. The carbon electrode was formed through two charge/discharge cycles before the measurement was conducted in order to eliminate irreversible capacity.

Table 1
Surface area, average pore size, type and manufacture for the activated carbon materials used in this study

Carbon	Total surface area ($m^2\ g^{-1}$)	Average pore size (Å)	Type	Manufacture
APD	941.1	31.6	Powder	Calgon
m20	1450	22.9	Powder	Spectrocorp (USA)
M1470	783	54.6	Powder	Norit
Nor-A	1211	24.6	Powder	Norit
PWA	718	36.9	Powder	Calgon
WPH	904	31.9	Powder	Calgon
U-1B	631	35.6	Cloth	Emtech (Canada)
U-2B	1179.4	28.1	Cloth	Emtech (Canada)
U-6B	957.5	36.1	Cloth	Emtech (Canada)
U-11B	1349	28.8	Cloth	Emtech (Canada)
U-L1-I3	1437.1	28.5	Cloth	Emtech (Canada)
U-T2	996.1	38.6	Cloth	Emtech (Canada)
U-T13	755.7	45.7	Cloth	Emtech (Canada)

An EG&G 170 potentiostat/galvanostat controlled by the Q&R Smart Data package was used for electrochemical measurements. A Micromeritics ASAP 2020 porosimeter was used for the surface area and porosity measurements. Nitrogen was used as absorbent gas. Density function theory (DFT) software from Micromeritics was also used. Siemens D5000

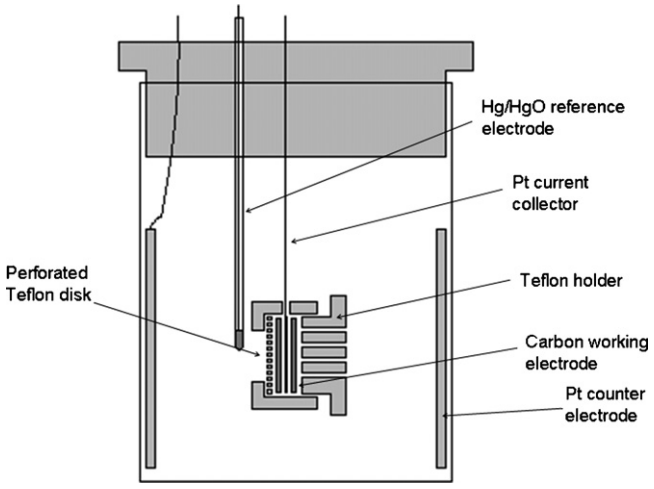

Fig. 1. Electrochemical cell used in the experiments.

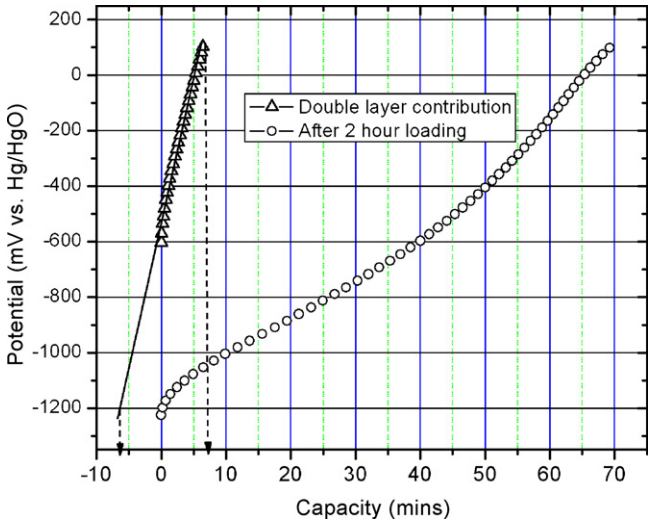

Fig. 2. Discharge of stored hydrogen, double-layer contribution.

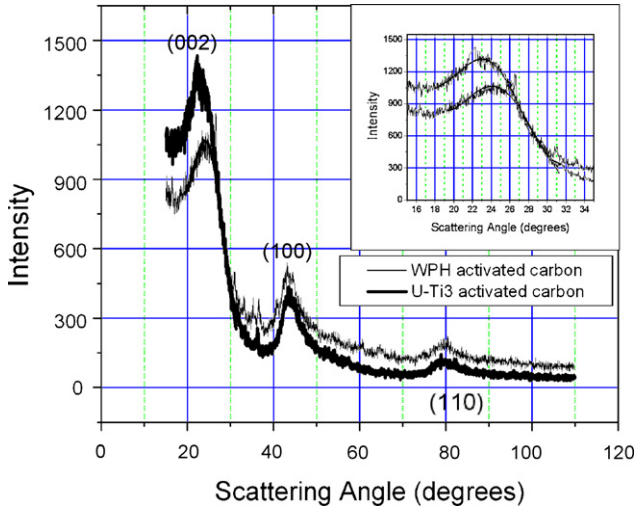

Fig. 3. XRD for WPH and U-Ti3 activated carbon. The enlargement of (0 0 2) peaks and fittings are shown in the inset.

powder diffractometer (XRD) equipped Cu target X-ray tube and monochrometer was used for all X-ray diffraction measurements.

3. Results and discussion

3.1. Impact of double-layer capacitance

When dc voltage is applied to the interface of an electrode, an electric double-layer is then established to store electrical energy. The electrical capacitance stored in the layer is proportional to the surface area of the electrode and 1/thickness of the double-layer. In a strong and concentrated electrolyte solution, a double-layer has a thickness of only a few angstroms. The electrodes used in the electrochemical hydrogen storage studies were made of high surface area carbon materials, so the contribution of the double-layer has to be considered in order not to inflate the electrochemical hydrogen storage capacity. Fig. 2 shows the impact of the double-layer. The electrode was first charged to −800 mV versus Hg/HgO, which is below hydrogen under potential deposition (UPD) potential. The charges were all used to charge the double-layer. The electrode was then discharged to release the charges stored in the double-layer, then the contribution of the double-layer for the electrode capacity could be calculated, as shown in Fig. 2. The double-layer contribution was subtracted for all the hydrogen capacity reported in this paper.

3.2. X-ray diffraction patterns and d_{002} calculation

Fig. 3 shows the typical XRD patterns for the high surface area carbon materials used in these studies. The clear observation of (1 0 0) peak near 42° and (1 1 0) peak near 79° indicates that the activated carbons consist of small domains or ordered graphene sheets. The interlayer distance between the graphene sheets (d_{002}) was calculated from the scattering angle of (0 0 2) peak using the Bragg equation. The fittings of (0 0 2) peak are also shown in Fig. 3. The scattering angles for both (1 0 0) and (1 1 0) peaks remain the same for the two carbon materials, which confirms that the difference of the scattering angle of (0 0 2) peak did not result from sample displacement error. In a high surface area carbon material, a graphene sheet may only consist of a few carbon hexagons with dislocation, which may not be a planar sheet, as is the case with those in a graphite. The defective graphene sheets may stack together and form small domains with short-range order as shown in Fig. 6. When the organized regions contain a significant number of graphene sheets with no parallel neighbor, then strong background scattering develops at (0 0 2) peak position [27]. Owing to the strong scattering background, it is very difficult to accurately determine the d_{002} value for an activated carbon using the Bragg equation. However, it appears that the estimated d_{002} values could roughly represent the short-range structure of activated carbon. XRD patterns of all carbon samples are included in on-line supplementary information.

3.3. Electrochemical hydrogen adsorption

Fig. 4 shows the comparison of electrochemical oxidation of hydrogen stored in an activated carbon electrode after resting at different conditions. After the same amount of hydrogen was loaded through decomposition of alkaline electrolyte, the stored hydrogen was released through electrochemical oxidation after 10 s of rest, 48 h of rest at open circuit voltage (OCV) and 48 h rest at the constant potential of −1.250 V versus HgO/Hg. As shown in Fig. 4, half of the initially stored reversible hydrogen remained even after 48 h of rest at OCV.

Various carbon materials have unique pore distribution. The total surface of a fine powder comprises the walls of all pores. The information regarding the surface area and the porosity of the carbons was obtained through nitrogen adsorption isotherm using DFT. However, it is difficult to explain how electrochemically generated molecular H_2 could form a stable monolayer in ambient conditions in the porous structure of an activated carbon, as claimed in the literature [28], given the intrinsic difficulty for the carbon surface-H_2 van der Walls interaction to

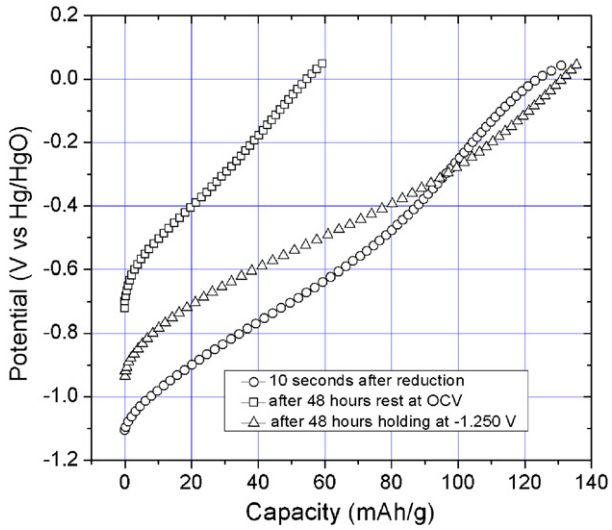

Fig. 4. Comparison of the oxidation of hydrogen electrochemically stored in M20 activated carbon electrode after resting at various conditions. Hydrogen was pre-loaded into the electrode by the reduction of 30 wt.% KOH electrolyte at 20 mA for 8 h. The weight of the electrode was 0.191 g. −1.25 V vs. Hg/HgO was 70 mV more positive than the hydrogen generation potential for the carbon electrode (−1.32 V).

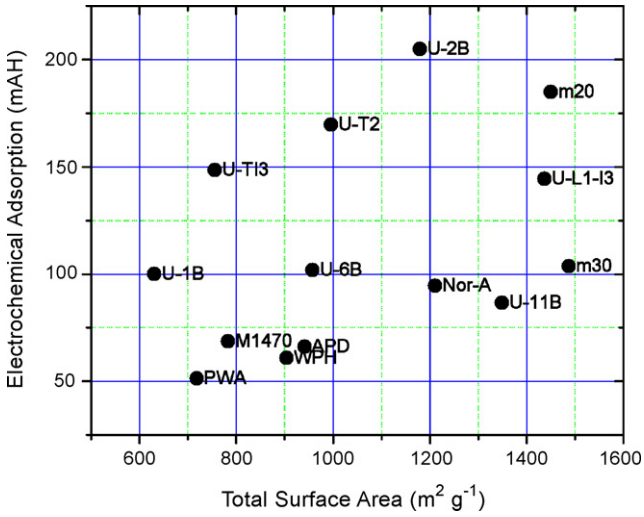

Fig. 5. Relationship between surface area and reversibly adsorbed hydrogen capacity.

compete with thermal energies. The process of hydrogen intercalation must always be distinguished from both physical and chemical surface adsorption. One of the characteristics of surface adsorption is that its capacity normally relates to the surface area of the material: the higher the surface area, the larger the amount of adsorption. Fig. 5 shows the relationship between the total surface area of the carbon materials and the amount of hydrogen reversibly adsorbed in them. No clear correspondence can be observed between the surface area and hydrogen electrochemical adsorption, which suggests that the majority of the hydrogen may not resist on the surface of carbon material. It is worth emphasizing that some electro-adsorbed hydrogen atoms would remain on the carbon surface and would reach a dynamic equilibrium with those inserted in the interlayer space.

It has been reported that H atoms from the dissociation of molecular hydrogen could intercalate into the graphite interlayer structure [29]. Fig. 6 illustrates the structure of the activated carbons and the possible mechanism for H insertion. The structure of defective graphene layer domains in the high surface area carbon provides the micro-units for the hydrogen accommodation. High surface area amorphous carbons consist of small hexagonal carbon rings, which are called “graphene layers”. Unlike the well ordered and planar graphene sheets in graphitized carbon, the sheets in the activated carbons are highly defective and may be curved. The carbons are made up of

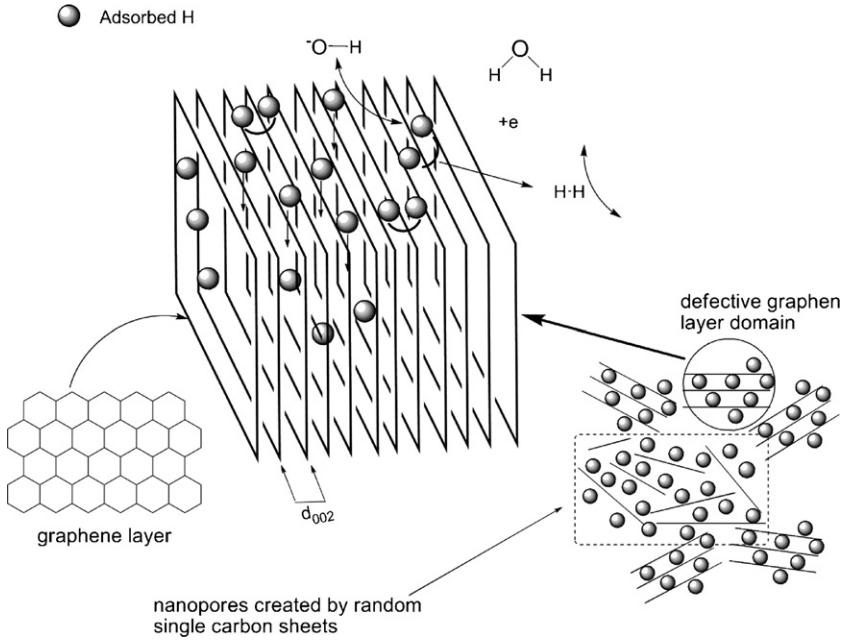

Fig. 6. Illustration of H electrochemical insertion into interlayer structure of microdomain of graphene layers.

associations, roughly parallel in structure and quite defective non-planar graphene sheets, like a "house of cards" [30]. Carbon materials made from different precursors and via different preparation methods have different size orientation and the stacking of their defective micro-graphene sheets is different. But in general, an activated carbon has an amorphous structure and lacks long-range three-dimensional order. An activated carbon can be considered as molecular space, this space being contained within a three-dimensional network of carbon atoms arranged in layers composed of range structures joined together somewhat imperfectly. This network is continuous in three dimensions, with some layers being stacked, roughly parallel to each other, in groups of two, or three, probably not much more [31]. Thus, the high surface area carbon materials are made up of randomly oriented single defective graphene sheets that contain appreciable nanoporosity with pores of the order of the size of graphene sheets and are stacked rather like a house of cards [32,33]. The majority of the electrochemically generated atomic hydrogen is proposed to reside in the interlayer space of defective graphene layers and the nanopores created by defective single carbon sheets of activated carbon. The minority of this hydrogen is chemically adsorbed onto the surface of either edge or basal orientations. The hydrogen on the edge orientation of the graphene layer domain is capable of diffusing into the interlayer space, while that adsorbed on the basal layer would remain on the surface. Due to the defective nature of the graphene sheets in amorphous carbon, the stable adsorption of atomic hydrogen on the basal layer would be at the sites of defect.

In the electrochemical reduction process, hydrogen atoms are formed at the surface of the electrode when the electrons transfer from the carbon electrode to H_2O molecules and are electrosorbed on the surface of the carbon electrode (Volmer reaction). $C(e) + H_2O \leftrightarrows CH_{ads} + OH^-$. There could be two competitive paths for the adsorbed H:

- Via desorptive recombination (Tafle reaction), $2CH_{ads} \leftrightarrows H_2 + C$ or "atom-ion" electrodesorption of H (Heyrovsky reaction), $CH_{ads} + C(e) + H_2O \leftrightarrows H_2 + OH^-$ [34].
- Followed by H intercalation/insertion into the lattice of host material, e.g. metal alloy or interlayer of carbon.

In the electrochemical oxidation process, H residing in the interlayer diffuses to the surface of the carbon electrode, gives one electron to the carbon host electrode, combines with an OH^- ion and forms H_2O. $CH_{ads} + OH^- \rightarrow C(e) + H_2O$. The H intercalation reaction would be the dominant reaction at low surface coverage of electrosorbed H, since the rate of H_2 evolution is proportional to the degree of H monolayer coverage on the electrode surface. The intercalation process goes on until the majority of the surface is covered with a monolayer of electrosorbed H, when a significant amount of H_2 starts to be generated. Fig. 7 shows the relationship between galvanostic discharge/charge efficiency, the hydrogen adsorption capacity (mAh g^{-1}) with the charging capacity. It is clearly demonstrated that the discharge/charge efficiency decreases with increasing charging capacity, even though the net discharge capacity increases with the charging capacity.

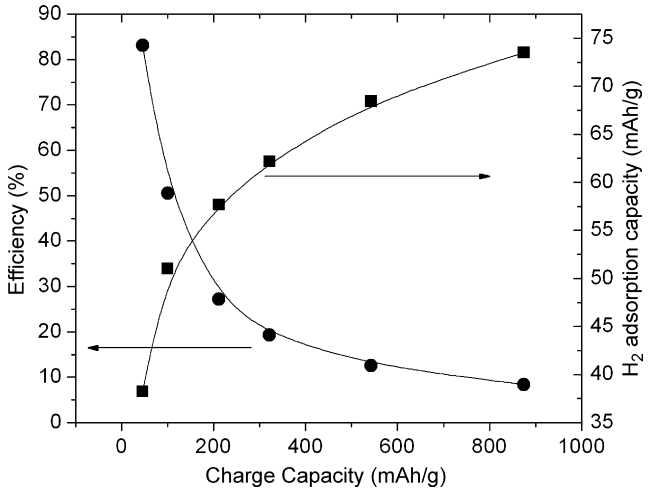

Fig. 7. Discharge and charge efficiency for hydrogen insertion. The electrode was made with M1470 activated carbon. The electrode was charged (reduction) at 100 mA g^{-1} current density and discharged (oxidation) at 50 mA g^{-1} current density. The efficient was defined as the percentage of oxidation capacity against reduction capacity.

The phenomena could be explained by the fact that before electrosorbed H coverage reaches the critical point, the majority of the H atoms on the edge surface become intercalated into the carbon interlayer and remain chemically adsorbed on the surface of the carbon, so they can be oxidized in the discharge process. As the charging continues, more and more H atoms recombine with their neighbors, forming H_2, which will not contribute to the discharge capacity. When the surface of the electrode is 100% covered by electrosorbed H, the discharge capacity only increases slightly, due to the continuous H insertion into the interlayer. The self-discharge phenomenon illustrated in Fig. 4 can also be explained by the proposed mechanism. During the rest at OCV, the intercalated H can gradually diffuse to the surface of the electrode and become surface adsorbed H; two of the neighboring H atoms could then recombine to form molecular hydrogen, which subsequently escapes from the electrode surface. Apparently, the H self-diffusion and recombination processes are kinetically slow; almost half of the original inserted H was preserved after 48 h of storage. It is interesting to note that after the carbon electrode was held at the constant potential, which was slightly more positive than the hydrogen generation potential for 48 h, the total hydrogen capacity did not change but the profile of the electrochemical oxidation curve changed. Since the resting potential was more positive than the water electrolysis potential, there was no additional atomic H being produced. Unlike the self-discharge (leakage of hydrogen) of the hydrogen loaded electrode resting at OCV, almost all the existing H was preserved in the carbon structure due to the fact that the adsorbed H atoms are strongly electrosorbed by the applied potential. It seems that instead of diffusion and recombination to form molecular hydrogen, the surface adsorbed H atoms and intercalated H atoms in the interlayer were allowed to redistribute to reside at more energy favorable locations in the carbon structure during the rest at static potential. This demonstrated through the profile change for the hydrogen oxidation

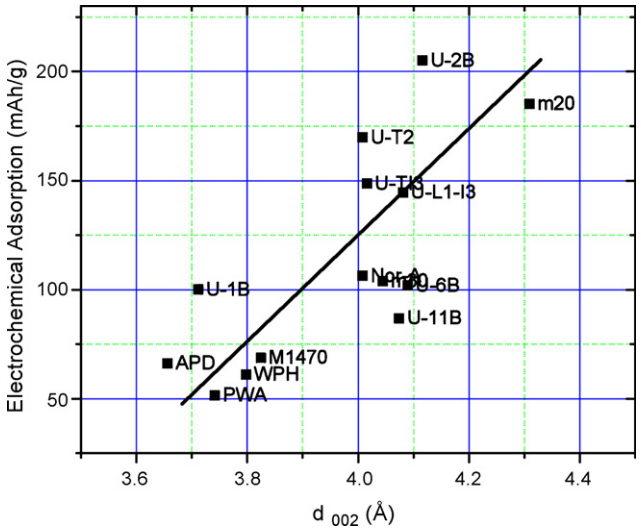

Fig. 8. The relationship between the interlayer distance of defective graphene sheets (d_{002}) measured by (0 0 2) XRD peak and the Bragg equation, and the electrochemical adsorption of hydrogen.

curves before and after resting at −1.250 V in Fig. 4. The phenomenon is critical for efficient hydrogen storage in the carbon materials. The static potential applied to the hydrogen loaded electrode can be used as a hydrogen release valve. The valve is closed when static potential is applied to the charged electrode and the H atoms intercalated in the carbon structure are confined in the framework of carbon electrode for a prolonged storage.

According to the proposed mechanism as shown in Fig. 6, the structure of carbon material should have an impact on the amount of hydrogen stored in the interlayer and nanopores. After forming surface adsorbed H atoms, they can further diffuse into the bulk of the carbon host structure, occupying sites with higher adsorption energy; the process is strongly dependent on the interlayer distance and the size of nanopores created with single graphene layers. Fig. 8 shows the relationship between hydrogen storage capacities and the interlayer space, d_{002}. The interlayer spacing was roughly estimated from an (0 0 2) X-ray diffraction peak by the Bragg equation. As shown in Fig. 8, the electrochemical hydrogen adsorption in the carbon materials is apparently related to the interlayer distance (d_{002}); the amount of hydrogen stored increases with the increase of d_{002}. In general, the intercalation must initially find exposed graphene edges, and these sites then provide pathways for more H atoms to move inward, filling the space between the basal planes. A large interlayer space could provide a better pathway for H diffusion, thus make the inner space of the defective graphene sheet domains more accessible for H atoms. This suggests that the H atoms are located in the defective carbon layers, including the stacked carbon layer domains and the nanoporosity created by randomly ordered single layers.

4. Conclusion

Electrochemical hydrogen storage in various high surface area carbon materials has been studied. The majority of atomic hydrogen generated through electrolysis was found to be intercalated into the interlayer spaces of the microdomains of defective graphene sheets, while the minority were electrochemically adsorbed onto the carbon surface. The total capacity of hydrogen storage is proportional to the interlayer distance and not to the carbon specific surface area. Static potential imposed on a hydrogen loaded carbon electrode could act as an electrochemical valve to retain the hydrogen within the carbon microstructure for prolonged storage.

Acknowledgements

Financial support granted by UMass Boston through Joseph P Healey Grant is gratefully acknowledged.

Appendix A. Supplementary data

Supplementary data associated with this article can be found, in the online version, at doi:10.1016/j.jpowsour.2007.12.098.

References

[1] X. Zhao, B. Xiao, A.J. Fletcher, K.M. Thomas, D. Bradshaw, M.J. Rosseinsky, Science 306 (2004) 1012–1015.
[2] A. Zaluska, L. Zalushi, J.O. Strom-Olsen, Appl. Phys. A 72 (2001) 157–165.
[3] V.Z. Mordkovich, N.N. Korostyshevsky, Y.K. Baichtock, N.V. Dudakova, V.P. Mordovin, M.H. Sosna, Int. J. Hydrogen Energy 18 (1993) 747–749.
[4] R.L. Cohen, J.H. Wernick, Science 214 (1981) 1081–1087.
[5] S. Giselle, Electrochem. Soc. Interf., Fall (2004) 40–45.
[6] G. Sandrock, J. Alloys Compd. 293-295 (1999) 877–888.
[7] G. Sandrock, R.C. Bowman Jr., J. Alloys Compd. 356–357 (2003) 794–799.
[8] S. Orimo, Y. Nakamori, A. Zuttel, Mater. Sci. Eng. B108 (2004) 51–53.
[9] Y. Kojima, Y. Kawai, H. Nakanishi, S. Matsumoto, J. Power Sources 135 (2004) 36–41.
[10] A. Zuttel, P. Wenger, S. Rentsch, P. Sudan, Ph. Mauron, Ch. Emmenegger, J. Power Sources 118 (2003) 1–7.
[11] W. Mao, H.-K. Mao, A.F. Goncharov, V.V. Struzhkin, Q. Guo, J. Hu, J. Shu, R.J. Hemley, M. Somayazulu, Y. Zhao, Science 297 (2002) 2247–2249.
[12] P. Chen, Z. Xiong, L. Lou, J. Lin, K.L. Tan, Nature 420 (2002) 302–304.
[13] E. Frackowiak, F. Beguin, Carbon 40 (2002) 1775–1787.
[14] C. Vix-Guterl, E. Frackowiak, K. Jurewicz, M. Friebe, J. Parmetier, F. Beguin, Carbon 43 (2005) 1293–1302.
[15] S.R. Ovshinsky, M.A. Fetcenko, J. Ross, Science 260 (1993) 176–181.
[16] K. Jurewicz, E. Frackowiak, F. Beguin, Appl. Phys. A 78 (2004) 981–987.
[17] A. Zuttel, P. Wenger, P. Sudan, P. Mauron, S.L. Orimo, Mater. Sci. Eng. B204 (2004) 9–18.
[18] C. Zutzenadel, A. Zuttel, D. Chartouni, L. Schlapbach, Electrochem. Solid State Lett. 2 (1999) 30–32.
[19] X. Qin, X.P. Gao, H. Liu, H.T. Yuan, D.Y. Yan, W.L. Gong, D.Y. Song, Electrochem. Solid State Lett. 3 (2002) 532–535.
[20] N. Rajalakshmi, K.S. Dhathathreyan, A. Govindaraj, B.C. Satishkumar, Electrochim. Acta 45 (2000) 4511–4515.
[21] G. Gundiah, A. Govindaraj, N. Rajalakshmi, K.S. Dhathathreyan, C.N.R. Rao, J. Mater. Chem. 13 (2003) 209–213.
[22] K. Jurewicz, E. Frackowiak, F. Beguin, Electrochem. Solid-State Lett. 4 (2001) A27–A29.
[23] K. Jurewicz, E. Frackowiak, F. Beguin, Fuel Process. Technol. 77–78 (2002) 415–421.
[24] D.Y. Qu, J. Power Sources 109 (2002) 403–411.
[25] D.Y. Qu, H. Shi, J. Power Sources 74 (1998) 99–107.
[26] M. Watanabe, M. Tachikawa, T. Osaka, Electrochim. Acta 42 (1997) 2707–2716.

[27] W. Xing, J.S. Xue, T. Zheng, A. Gibaud, J.R. Dahn, J. Electrochem. Soc. 143 (1996) 3482–3491.
[28] A. Zuttel, P. Sudan, Ph. Mauron, T. Kiyobayashi, Ch. Emmeregger, L. Schlapbach, Int. J. Hydrogen Energy 27 (2002) 203–212.
[29] D.L. Browing, M.L. Gerrand, J.B. Lakeman, I.M. Mellor, R.J. Mortmer, M.C. Turpin, Nano Lett. 2 (2002) 201–205.
[30] X. Liu, J.X. Xue, T. Zheng, J.R. Dahn, Carbon 34 (1996) 193–200.
[31] H. Marsh, F. Rodeigues-Reinoso, Activated Carbon, Elsevier, New York, 2006, p. 71.
[32] W.B. Xing, J.S. Xue, T. Zheng, A. Gibaud, J.R. Dahn, J. Electrochem. Soc. 143 (1996) 3482–3491.
[33] J.R. Dahn, T. Zheng, Y. Liu, J.S. Xue, Science 270 (1995) 590–593.
[34] J.O'M. Bockris, A.K.N. Reddy, Modern Electrochemistry, vol. 2, Plenum Press, New York, 1970.